



## Novel Ni-based FI catalyst for ethylene polymerization

Saman Damavandi<sup>a</sup>, Narjes Samadieh<sup>a</sup>, Saeid Ahmadjo<sup>b</sup>, Zahra Etemadnia<sup>a</sup>,  
Gholam Hossein Zohuri<sup>a,\*</sup>

<sup>a</sup> Department of Chemistry, Faculty of Science, Ferdowsi University of Mashhad, Mashhad, Iran

<sup>b</sup> Department of Catalyst, Iran Polymer and Petrochemical Institute, Tehran, Iran

### ARTICLE INFO

#### Article history:

Received 13 January 2014

Received in revised form 20 December 2014

Accepted 23 December 2014

Available online 8 January 2015

#### Keywords:

Late transition metal catalyst

Nickel catalyst

Naphthoxy-imine ligand

Polymerization

Polyethylene

### ABSTRACT

Novel nickel based FI catalysts with different ligands from well known salicylaldehyde imine ligand, to naphthoxy-imine ligand were designed, synthesized, and characterized. The effect of synthesized ligand on ethylene polymerization was investigated. Extensive experimentations have been carried out using the nickel catalysts after activation with methylaluminoxane (MAO) to study the ethylene polymerization behavior of the prepared catalysts comparably. Substituents on the arene moiety and/or the backbone of the ligand influence the activities of the active sites of the catalyst during the polymerization. Therefore, not only polymerization behavior varied, but also versatile products regarding molecular weight, crystallinity and melting point were obtained. The crystallinities and melting points of the polymer obtained at the temperatures of 10, 30 and 60 °C were 58%, 39%, and 14% and 130, 97 and 88 °C respectively.

© 2015 Elsevier Ltd. All rights reserved.

### 1. Introduction

From the metallocenes to post-metallocenes and then to late transition metal catalysts, a series of landmarks can be defined during the chronological development of the homogeneous olefin polymerization catalysts. These include the bis(cyclopentadienyl) titanium or zirconium dichloride [1–5], the C<sub>2</sub> symmetrical *rac*-ethylenebis(indenyl)titanium dichloride (isotactic PP) [6–8], the C<sub>s</sub> symmetrical isopropyl(cyclopentadienyl-1-fluorenyl)zirconium dichloride (syndiotactic PP) [9], the *ansa*-cyclopentadienyl-amide titanium or zirconium dichlorides (constrained geometry catalysts, CGC) (ethylene/ $\alpha$ -olefin copolymers) [10–12], the  $\alpha$ -diimine nickel(II) and palladium(II) dihalides (branched polyethylenes (PE)) [13], the 2,6-bis(imino)pyridine iron(II) and cobalt(II) dihalides (linear PE) [14–16], the phenoxy-imine-based Group 4 transition metal catalysts (FI catalysts) (living polymerization of ethylene and propylene)

[17] and the neutral single component salicylaldehyde-based nickel (II) alkyl or aryl catalysts [18]. From the comparison of these different homogeneous catalysts, one can observe that they are based on a limited number of metals (Ti, Zr, Hf, Fe, Co, Ni, Pd), therefore, the main differences lying on the diversity of their ligands. Additionally, it can be observed that only when a particular ligand set combines with a certain metal a desirable catalytic activity is promoted, whereas many other ligands may fail. The reason why it happens is still remains a mystery, which is in fact one of the driving forces for further research in the development of new and high performance catalysts. Coordination of a ligand to a metal not only alters its basic physical and chemical properties, such as color, solubility, stability, and symmetry, but also affects its electronic distribution and coordination environment leading to varied electronic, magnetic and catalytic properties [19].

It is worth to note that, sometimes, the ligands can also influence the catalytic performances of the catalysts in olefin polymerization through the establishment of non-bonded interactions of the ligands with the growing

\* Corresponding author. Tel.: +98 2148662474.

E-mail address: [zohuri@um.ac.ir](mailto:zohuri@um.ac.ir) (G.H. Zohuri).

polymer chains, which are coordinated to the metal centers. For instance, our previous research revealed that FI catalysts containing fluorinated aryl phenoxy-imine chelate ligands demonstrated to induce unprecedented living polymerization effects with both ethylene and propylene, through an attractive interaction between one of the fluorine atoms in the ligand and a  $\beta$ -hydrogen atom on the growing polymer chain [20].

Due to the significance and versatility of the ligands in the homogeneous olefin polymerization catalysts, the design of the precatalysts is mainly focused on the design and modification of the ligand itself. A large amount of work has been devoted to the modification of FI (Phenoxy-imine) ligand and to the understanding of the chemistry of its metal derivatives, these subjects being addressed in reviews published recently [21–23]. Presence of the N,O-heteroatoms coordinating FI ligands makes the complex more electrophilic renders the M–L bonding properties of the FI catalysts more ionic or polarized relative to other mentioned catalysts, which may cause the stronger affinity to inorganic surfaces and the higher tolerance to polar functionalities of the FI catalysts. A literature survey indicates that the FI ligands are mostly coordinated to the transition metals, such as titanium, zirconium, hafnium and vanadium [24–26], while less attention has been paid to the FI nickel-based catalysts [27–29]. Therefore, in the present study, following to our recent research considering the principles to design FI ligands [30–33], nickel based FI catalysts have been synthesized and applied for ethylene polymerization. Herein, we wish to report the details of this study.

## 2. Experimental

### 2.1. Materials

Dimethoxyethanenickel dibromide, dichloromethane, methanol, *p*-toluenesulfonic acid (*p*-TSA), phenol and phenol derivatives were supplied by Merck Chemical (Darmstadt, Germany) and were used as received. Paraformaldehyde, 3.0 M Ethylmagnesium bromide in diethylether, 1.6 M *n*-Butyllithium in hexane were purchased from Aldrich Chemical Company and used as received. Toluene was obtained from Merck Chemicals, *n*-hexane was supplied by Arak Petrochemical Co (Arak, Iran), the chemicals were prepared from distilling over sodium wire, stored over 13X and 4A activated molecular sieves and degassed by bubbling with dried nitrogen gas before use. Polymerization grade ethylene (purity 99.9%) was supplied by Iranian Petrochemical (Tehran, Iran). Nitrogen gas (purity 99.99%) was supplied by Roham (Tehran Iran). Methylaluminoxane (MAO) (10% solution in toluene) and Triisobutylaluminum (TIBA) (purity 93%) was supplied by Sigma Aldrich Chemicals (Steinheim, Germany).

#### 2.1.1. Ethylene polymerization

The polymerization was performed in a stainless steel Buchi reactor size 1 L equipped with an agitator. The reactor was evacuated and purged with N<sub>2</sub> several times at 110 °C for removing of oxygen and moisture. Toluene was added into the reactor at room temperature and saturated with ethylene gas. TIBA was used as scavenger and added to the

reactor before addition of the MAO. Following to, various MAO and catalyst ration were added respectively with stirring at 800 rpm under specific ethylene pressure. Ethylene gas feed was started and the pressure of reactor was kept constant at the applied monomer pressure for each run. At the end of the polymerization, the residue ethylene gas was released out of reactor and the polymer slurry was quenched with acidic ethanol. The polymer was filtrated, washed with ethanol and dried in vacuum oven at about 60 °C for 8 h.

#### 2.1.2. Polyethylene and complex characterization

<sup>1</sup>H NMR spectrum was recorded on a Bruker BRX-100 AVANCE spectrometer. Elemental analysis for CHN was carried out by CHNO type Thermo Firingan 1112 EA microanalyzer. Differential scanning calorimetry (DSC) (Universal V4IDTA) with a rate of 10 °C/min was used for the PE characterization. The degree of crystallinity of a polyethylene sample can be calculated from its heat of fusion which can be determined by differential scanning calorimetry [34]. Calculation of  $\Delta H_f/\Delta H_f^0 \times 100$  gives the values of crystallinity where  $\Delta H_f$  is the heat of fusion and  $\Delta H_f^0 = 69$  cal/g is the heat of fusion of 100% crystalline polyethylene. Intrinsic viscosity  $[\eta]$  was measured in decaline at 135 °C using an Ubbelohde viscometer.  $M_v$  values were calculated through equation  $[\eta] = 6.2 \times 10^{-4} M_v^{0.7}$  [35]. All the catalyst preparation and polymerization procedure were carried out under dried N<sub>2</sub>.

### 2.2. Synthesis of 2-hydroxy-1-naphthaldehyde

The procedure was used according to Ref. [36]. To a stirred solution of  $\beta$ -naphthol (2 mmol) in ethanol (30 mL) a solution of sodium hydroxide (10 mmol) in water (50 mL) was added. The resulting solution was heated to 80 °C and chloroform (2.4 mmol) was added via dropping funnel over a period of 1–1.5 h. The ethanol and excess chloroform were removed and hydrochloric acid was added dropwise to the residue in order to neutralize the excess sodium hydroxide and to liberate the phenolic aldehyde from its sodium salt. After filtration of sodium chloride, the residue was distilled under reduced pressure. The obtained colored oily distillate solidified on cooling. Recrystallization of the solid using ethanol obtained the 2-hydroxy-1-naphthaldehyde in a moderate yield (51%).

#### 2.2.1. Synthesis of 1-[(phenyl)imino]methyl-2-naphthol

To a stirred mixture of 2-hydroxy-1-naphthaldehyde (10 mmol) in methanol (30 mL), aniline (11 mmol) was added over a 5 min time at reflux condition in the presence of trace amount of *p*-toluenesulfonic acid as the catalyst. The reaction was monitored by TLC and after disappearance of the initial compounds, the solvent was removed and the solid product was purified by recrystallization from ethanol. The yield of the reaction was about 90%. <sup>1</sup>H NMR (CDCl<sub>3</sub>):  $\delta$  7.07 (dd, 1H), 7.10 (d, 1H), 7.17 (d, 2H), 7.46 (d, 2H), 7.68 (m, 3H), 7.93 (d, 1H), 8.05 (d, 1H), 8.42 (s, 1H, CH=N), 12.40 (brs, 1H, OH). Anal. Calcd. for C<sub>17</sub>H<sub>13</sub>NO: C, 82.57; H, 5.30; N, 5.66. Found: C, 82.51; H, 5.33; N, 5.62.

### 2.2.2. Preparation of catalyst **1**

Dimethoxyethanenickel dibromide (DME)NiBr<sub>2</sub> (1.2 mmol) and ligand **1** (1.2 mmol) were combined in a Schlenk flask under a nitrogen atmosphere to prepare Ni-based FI catalyst **1** (Scheme 1). CH<sub>2</sub>Cl<sub>2</sub> (25 mL) was added to the solid mixture. The produced suspension was stirred for 12 h at room temperature. Solvent removal of the suspension resulted in formation of a brown solid. The solid was washed with Et<sub>2</sub>O several times and dried in vacuum. The yield of the reaction was about 70%; mp: >300 °C. NMR characterization was not possible because the compound is paramagnetic. Anal. Calcd. For C<sub>17</sub>H<sub>12</sub>NONiBr: C, 53.05; H, 3.14; N, 3.64. Found: C, 53.16; H, 3.18; N, 3.69. EIMS: MS (*m/z*): 386 (M+2), 384 (M), 304 (M–Br), 246 (M–NiBr).

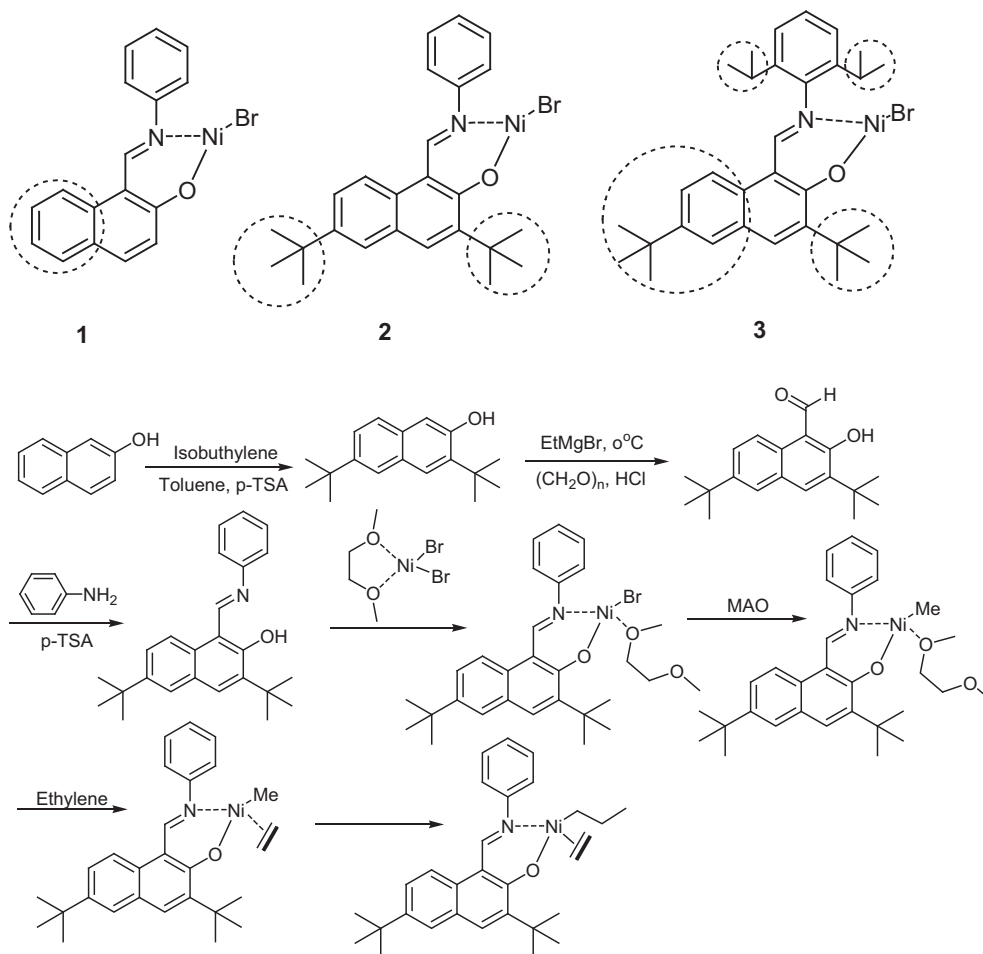
### 2.3. Synthesis of 3,6-di-tert-butyl-2-naphthol

The 3,6-di-tert-butyl-2-naphthol were prepared according to the literature [37]. 2-Naphthol (60 g, 0.42 mole), *p*-TSA (12 g, 0.063 mole), and toluene (200 mL), were added to a 500 mL three-necked round bottom flask, equipped with stirrer bar, thermometer and gas bubbler. The mixture was heated to 110 °C, and isobutylene gas was bubbled through the solution slowly (150 bubbles per min). After

two weeks, the reaction was quenched by adding 700 mL water. Toluene was added (200 mL) to dissolve the precipitated material, and the layers were separated. The toluene layer was isolated and dried over MgSO<sub>4</sub>. Subsequent removal of toluene under reduced pressure and recrystallization from hexane resulted in pure product. The product was isolated as white powder, yield 25%. <sup>1</sup>H NMR (CDCl<sub>3</sub>): 1.43 (s, 9H), 1.56 (s, 9H), 5.10 (s, 1H), 6.85–7.57 (m, 3H), 7.70 (s, 2H). Anal. Calcd. for C<sub>18</sub>H<sub>24</sub>O: C, 84.32; H, 9.44. Found: C, 84.38; H, 9.51%.

### 2.3.1. Synthesis of 3,6-di-tert-butyl-2-hydroxy-1-naphthaldehyde

To a stirred ethylmagnesium bromide (3.0 M in Et<sub>2</sub>O, 30 mmol) a solution of 3,6-di-tert-butyl-2-naphthol (in THF, 28.0 mmol) was added dropwise over a 15 min at 0 °C. The mixture was stirred for 2 h at room temperature. Dried toluene (50 mL) and a mixture of triethylamine (41.6 mmol) and paraformaldehyde (purity 94%, 93.9 mmol) were added. The mixture was stirred for further 2 h at 80 °C. HCl (6 N, 20 mL) was added at 0 °C. The organic phase was separated, dried over MgSO<sub>4</sub> to obtain the product (yield 76%). <sup>1</sup>H NMR (CDCl<sub>3</sub>, 100 MHz): δ 1.21 (d, 9H), 1.32 (d, 9H), 7.45–7.80 (m, 4H), 10.15 (s,



**Scheme 1.** Structure of the synthesized FI-Ni based catalysts **1–3** and synthetic route to synthesize catalyst **3**.

1H, CHO), 12.85 (bs, 1H, OH). Anal. Calcd. for  $C_{19}H_{24}O_2$ : C, 80.24; H, 8.51. Found: C, 80.18; H, 8.55%.

### 2.3.2. Synthesis of 1-[phenylimino]methyl-3,6-ditert-butyl-2-naphthol

The FI ligand preparation was carried out according to the method used in Section 2.2.1. The ligand was obtained as yellow solid with the yield of 81%.  $^1H$  NMR ( $CDCl_3$ , 100 MHz):  $\delta$  1.40 (s, 9H), 1.63 (s, 9H), 6.84–7.21 (m, 5H), 7.31–7.65 (m, 4H), 8.22 (s, 1H, CH=N), 12.18 (brs, 1H, OH). Anal. Calcd. for  $C_{25}H_{29}NO$ : C, 83.52; H, 8.13; N, 3.90. Found: C, 83.43; H, 8.17, N, 3.94%.

### 2.3.3. Preparation of catalyst 2

The Ni-based FI catalyst **2** (Scheme 1) was synthesized according to the procedure mentioned in Section 2.2.2. The yield of the reaction was about 73%; mp: >300 °C. Anal. Calcd. For  $C_{25}H_{28}NONiBr$ : C, 60.40; H, 5.68; N, 2.82. Found: C, 60.31; H, 5.64; N, 2.85. EIMS: MS ( $m/z$ ): 497 (M+2), 495 (M), 416, (M–Br), 358 (M–NiBr).

### 2.4. Synthesis of 1-[2,6-diisopropylphenylimino]methyl-3,6-ditert-butyl-2-naphthol

The FI ligand preparation was carried out according to the method used in Section 2.2.1. The ligand was obtained as yellow solid with the yield of 85%.  $^1H$  NMR ( $CDCl_3$ , 100 MHz):  $\delta$  1.30 (d, 12H), 1.42 (s, 9H), 1.68 (s, 9H), 3.35 (m, 2H), 6.80–7.15 (m, 4H), 7.55–7.80 (m, 3H), 8.15 (s, 1H, CH=N), 12.44 (bs, 1H, OH). Anal. Calcd. For  $C_{31}H_{41}NO$ : C, 83.92; H, 9.31; N, 3.16. Found: C, 83.83; H, 9.28, N, 3.19%.

### 2.4.1. Preparation of catalyst 3

The Ni-based FI catalyst **3** (Scheme 1) was synthesized according to the procedure mentioned in Section 2.2.2. The yield of the reaction was about 73%; mp: >300 °C. Anal. Calcd. For  $C_{31}H_{40}NONiBr$ : C, 64.06; H, 6.94; N, 2.41. Found: C, 64.01; H, 6.99; N, 2.45. EIMS: MS ( $m/z$ ): 581 (M+2), 579 (M), 500 (M–Br), 442 (M–NiBr).

## 3. Results and discussion

The general structure of the catalysts used in this study is shown in Scheme 1. They were prepared by the conventional Schiff-base condensation of 1 equiv. of the desired substituted anilines with the prepared naphthaldehyde. The pre-catalysts were formed by addition of the ligands to  $(DME)NiBr_2$ . The reactions were complete in all cases in less than 12 h, and the products are isolated by filtration or evaporation and washed with ether to yield the desired catalyst precursors in quantitative yields.

The experiments of ethylene polymerization with catalysts **1–3** were carried out by dissolving the corresponding catalysts in toluene, followed by the injection of a toluene solution of different amount of TIBA, MAO and monomer gas in to the Buchi reactor. After 30 min, reactions were terminated by shutting off the feed stream, followed by nitrogen purge and polymer precipitation using acidified

(HCl) ethanol. The results of polymerization are listed in Table 1.

The initial data from the ethylene polymerization indicated that the catalyst **1** is almost inactive for ethylene polymerization while the catalysts **2** and **3** are capable to polymerize ethylene with moderate activities. Due to the low catalytic activity of the catalyst **1**, further studies have been devoted to the catalysts **2** and **3**.

Neither complexes **1** nor **2** and **3** could be used as single component catalyst to polymerize ethylene, while Grubbs' catalysts with bulky phenyl group nor can larger groups at the ortho position of the phenoxy group catalyze ethylene polymerization without cocatalyst [18]. It is clear that the prepared catalysts **1–3** are different from mononuclear Grubbs' catalysts.

Fig. 1 shows the relationships between polymerization conditions, activities and molecular weights of the obtained polyethylene. The ratio of  $[Al]/[Ni]$  is essential for the catalysts to polymerize ethylene. Variation of the molar ratio of  $[Al]/[Ni]$  showed considerable effects on the catalyst activities and molecular weights of the obtained polyethylene. Figs. 1 and 2 showed the catalyst behaviors over cocatalyst/catalyst molar ratios. Applying the catalyst **2** under 2 bar ethylene pressure, only trace product was obtained at 500:1 ratio, while activity of  $8.93 \times 10^3$  g PE/mmol Ni h was obtained when the  $[Al]/[Ni]$  ratio was increased to 1500:1. More increase of  $[Al]/[Ni]$  ration led to decrease of the activity. Therefore, the ratio of 1500:1 was chosen for further studies. At the  $[Al]/[Ni]$  ratio of 1500:1, catalyst **3** showed an activity of  $6.64 \times 10^3$  g PE/mmol Ni h, while the activity was linearly increased by addition of  $[Al]/[Ni]$  ratio up to 3000:1 which the activity reached to  $9.25 \times 10^3$  g PE/mmol Ni h. It is conceivable that coexistence of two bulky groups at the ortho position to the phenoxy oxygen and on the N atom of imine prevent the catalysts from coordination to the cocatalyst leading to easier ethylene insertion to the active centers (Scheme 2). On the other side, the propagation reaction occurs only when the complex formed by the cationic catalyst and MAO is dissociated. Accordingly, the metallic cation solvated by excess amount of MAO (Scheme 3) is expected to be more active than the contact ion pair causes better ion separation resulting in increasing the activity of the catalyst **3** to higher values [29–31].

Fig. 3 demonstrates the influence of the polymerization temperature on activity and polymer molecular weight obtained by catalyst **2**. Our results showed that polymerization temperature of 25–30 °C is the optimum for both catalysts from the aspect of activity of the catalytic system. However, above the optimum polymerization temperature, as demonstrated in Figs. 3 and 4, in comparison of catalysts **2** and **3**, the activity of the catalyst **3** was dramatically decreased. This may result from the deactivation process due to the poorer thermal stability of the cationic active centers of the catalyst **3**. The effect of temperature on catalyst activity might be explained by Brookhart theory on deactivation mechanism of  $\alpha$ -diimine catalysts [38]. The motion and rotation of aryl ring is increased at higher polymerization temperature. Therefore, due to the C–H bond activation of an ortho alkyl substituent, perturbation occurred in coordination step through a disorder in overlap

**Table 1**

Characterizations of the resulting polymers.

Pressure (bar)	Catalyst	Temperature (°C)	Activity (g PE/mmol Zr h)	Crystallinity (%)	$T_m$ (°C)	$M_v \times 10^4$
2	Catalyst 2	10	$4.4 \times 10^3$	58	130	17.21
2	Catalyst 2	30	$9.1 \times 10^3$	39	97	18.12
2	Catalyst 2	60	$4.1 \times 10^3$	14	88	7.60
4	Catalyst 2	30	$1.4 \times 10^4$	52	108	19.18
2	Catalyst 3	10	$5.5 \times 10^3$	60	130	44.11
2	Catalyst 3	30	$9.5 \times 10^3$	52	117	40.80
2	Catalyst 3	60	$1.4 \times 10^3$	36	110	31.11
4	Catalyst 3	30	$1.6 \times 10^4$	54	130	34.05
6	Catalyst 3	30	$2.1 \times 10^4$	54	131	36.13

Polymerization conditions:  $[Al]/[Ni]$  = optimum values,  $[Ni] = 7 \times 10^{-3}$  mmol, time = 15 min, toluene = 250 mL.

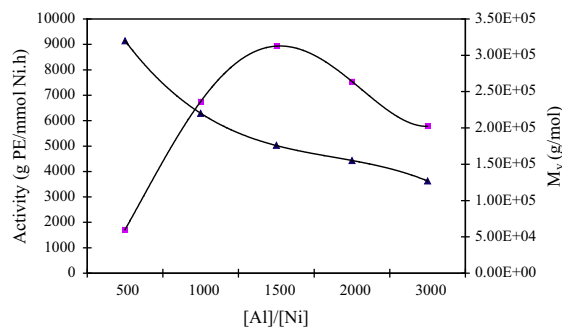


**Fig. 1.** Plots of activity (■) and  $M_v$  (▶) vs.  $[Al]/[Ni]$  for catalyst 2. Temperature = 25 °C, polymerization time = 15 min, monomer pressure = 2 bar,  $[Ni] = 7 \times 10^{-3}$  mmol, toluene = 250 mL.

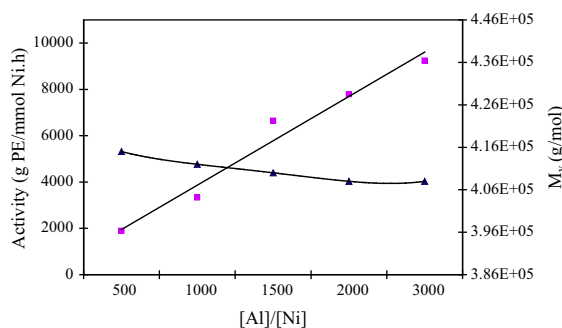
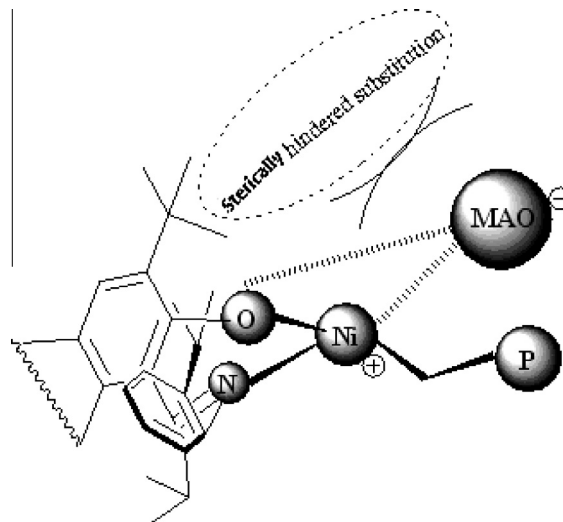


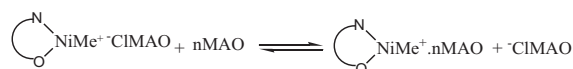
**Fig. 2.** Plots of activity (■) and  $M_v$  (▶) vs.  $[Al]/[Ni]$  for catalyst 3. Temperature = 25 °C, polymerization time = 15 min, monomer pressure = 2 bar,  $[Ni] = 7 \times 10^{-3}$  mmol, toluene = 250 mL.

of empty  $d$  orbital of the metal center with  $\pi$ -olefin orbital, leads to reduction of the activity of active centers [38].

The polymer molecular weight is the result of complex interplay of monomer insertion, chain transfer, and potential catalyst decomposition. For a stable catalyst, the polymer  $M_w$  is primarily controlled by the relative rates of monomer insertion and chain transfer ( $K_{ins}/K_{CT}$ ) [39]. Figs. 3 and 4 showed that the molecular weights of the polymers also depend on the polymerization temperature. As explained, a competition between the termination and propagation steps determines the molecular weight of the polymer. Higher polymerization temperatures increase



**Scheme 2.** Steric hindrance between bulky substitutions of the ligand and MAO in catalyst 2.



**Scheme 3.** Effect of MAO on ion pair separation and catalyst activation.

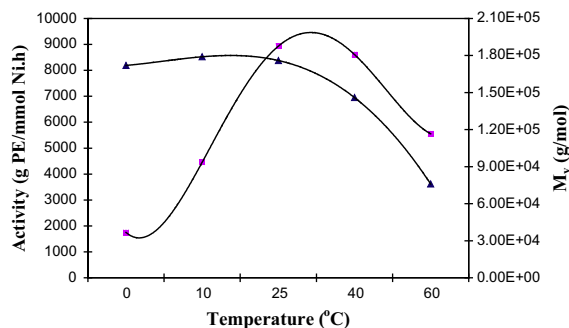


**Fig. 3.** Plots of activity (■) and  $M_v$  (▶) vs. reaction temperature for catalyst 2. Polymerization time = 15 min,  $[Al]/[Ni] = 1500:1$ , monomer pressure = 2 bar,  $[Ni] = 7 \times 10^{-3}$  mmol, toluene = 250 mL.

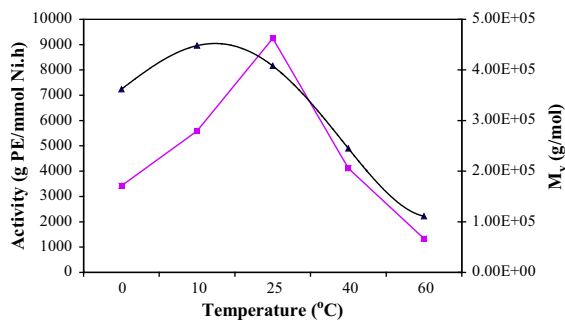
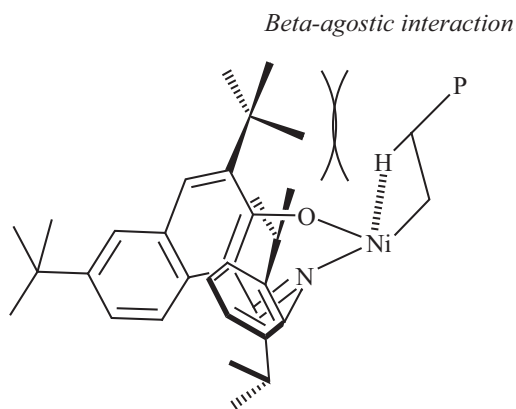


**Fig. 4.** Plots of activity (■) and  $M_n$  (▶) vs. reaction temperature for catalyst **3**. Polymerization time = 15 min,  $[Al]/[Ni] = 3000:1$ , monomer pressure = 2 bar,  $[Ni] = 7 \times 10^{-3}$  mmol, toluene = 250 mL.

the rate of  $\beta$ -hydride chain transfer which is over the propagation rate and affords a polymer with lower molecular weight. But, as can be seen in Fig. 4, molecular weight of the polymer obtained using catalyst **3**, is less sensitive to the polymerization temperature.

At the monomer pressure of 2 bars, ambient temperature and applying  $[Al]/[Ni] = 1500:1$  molar ratio, the prepared FI-Ni based catalysts **2** and **3** produced polyethylene with the  $M_n$  values of  $1.76 \times 10^5$  and  $4.1 \times 10^5$  respectively. As illustrated in Scheme 2, due to the oligomeric nature of MAO, the occurrence of a chain transfer reaction to MAO decreases as the bulkiness of the naphthoxy imine ligand increases. The relatively higher molecular weight of the polymer obtained using catalyst **3** must be due to lower chain transfer to MAO. Moreover, in catalyst **3** containing bulky isopropyl group phenyl ring on the nitrogen atom, it seems that the  $\beta$ -carbon of the polymer chain is not easily accommodated in the plane because of the steric interaction between naphthoxy-imine ligand of the catalyst and  $\beta$ -H of the growing polymer chain (Scheme 4). As a result,  $\beta$ -H elimination is suppressed leading to formation the polymer with higher molecular weight.

The kinetic behavior of the polymerization is shown in Fig. 5. Accordingly, activities of the catalysts increased to a maximum value of polymerization time. The maximum



**Scheme 4.**  $\beta$ -agostic steric repulsion interaction: steric repulsion between  $\beta$ -hydrogen of the growing polymer chain and alkyl substituents phenyl ring on the N in catalyst **3**.

activities of the catalysts were observed after 10 min of the polymerization for the reaction carried out under the optimized conditions of cocatalyst/catalyst ratio and temperature obtained for each catalyst already. As shown in Fig. 5, similar behavior was observed for the catalysts. In the early stage of the polymerization, the catalytic active centers are activated with MAO and lie easy to access the monomer, while with increasing of the polymerization time, the possibility of destruction of active centers increases and leads to the decreasing of the activities [30–33,35–37,18,38,39].

A dramatic effect on the crystallinity of the resulting polymer by catalyst **2** was observed with increasing of the polymerization temperature. The crystallinity and melting point of the polymers obtained by catalyst **2** at the polymerization temperatures of 10, 30 and 60 °C were 58%, 39%, and 14% and 130, 97 and 88 °C respectively (Table 1). At lower polymerization temperature due to the existence of bulky substitutions that block the axial position for transfer reactions, monomer insertion is favored, resulting in the formation of almost linear and semicrystalline polyethylene. However, at higher temperature the probable chain transfer reactions to the monomer resulted in the formation of fewer  $\alpha$ -olefin branches that we named them “monomer-like chains”. Frequent reinsertion of “monomer-like chains” to the C–H bond active centers leads to furnish branched PE with low melting points and low crystallinities. The mechanism of olefin branched polyethylene is illustrated in Scheme 5. This assumption can be confirmed by  $^{13}C$  NMR analysis to some extent.  $^{13}C$  NMR spectra (Fig. 6) showed that the products catalyzed by **2**/MAO showed corresponding branches’ resonance peaks including butyl and long branched chains ( $n \geq 6$ ) [40] which might be formed by reinsertion of short  $\alpha$ -olefins that we named “monomer-like chains”.

As illustrated in Scheme 5, alpha olefin trapping via 1,2 or 2,1 routs can occur within re-insertion of monomer lead to the introduction of branches in the polymer chain that is firmly confirmed by the observed peaks. Accordingly, the signals at 14.12, 14.65, 19.90, 20.02 and 33.29 ppm were corresponding to the signals of methyl branches indicating methyl branched PE [13,40–42]. The presence of the weak resonance at 31.21 ppm assigned to the paired 1,4 branches 1,4- $\alpha'$ B $_{n \geq 2}$ . n-propyl branch was identified by the signal

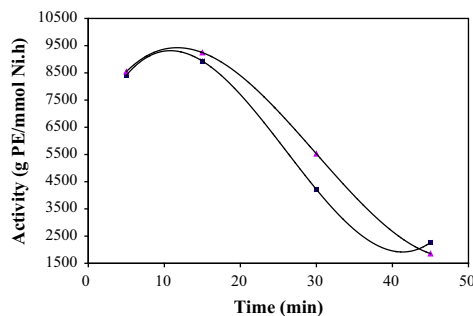
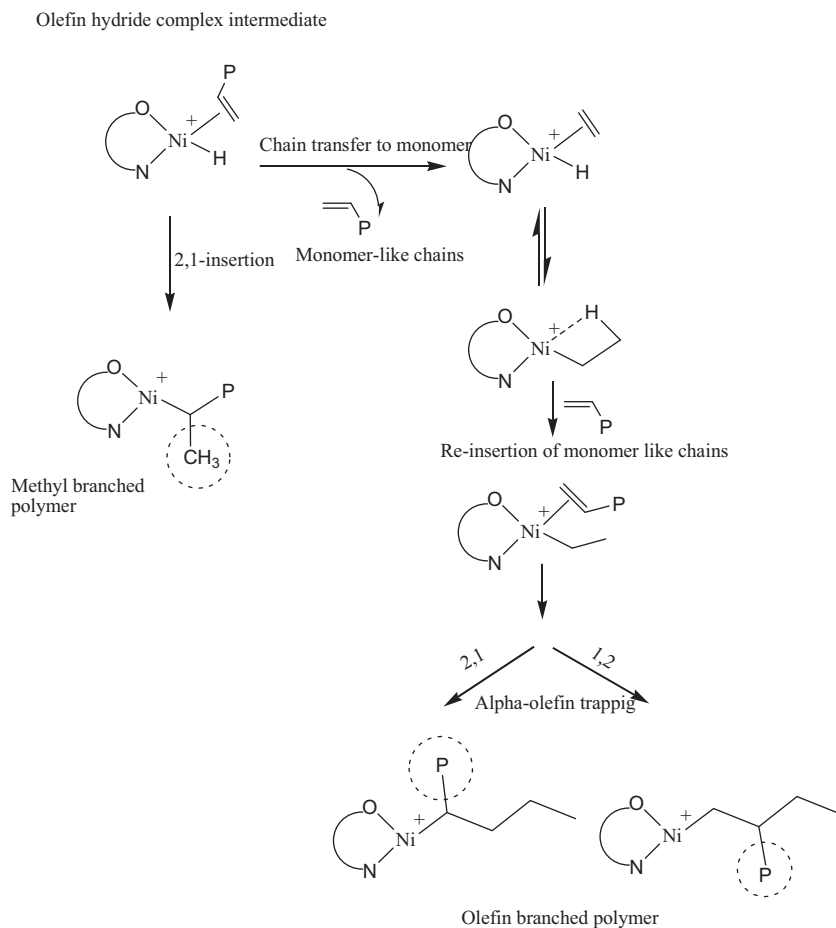


**Fig. 5.** Plots of activities of the catalysts **2** (■) and **3** (▶) vs. reaction time. Temperature = 25 °C,  $[Al]/[Ni]$  = optimum values, monomer pressure = 2 bar,  $[Ni] = 7 \times 10^{-3}$  mmol, toluene = 250 mL.



**Scheme 5.** Reasonable mechanistic route to formation of olefin branched polyethylene.

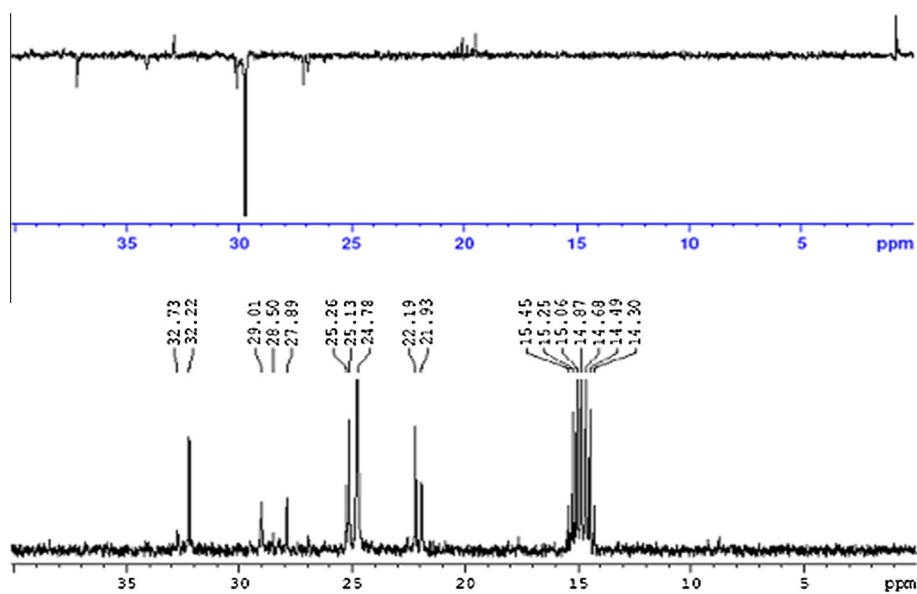


**Fig. 6.**  $^{13}\text{C}$  NMR spectrum of the PE obtained by 2/MAO.

appeared at 14.30 ppm [42]. Butyl branches were identified by signals at 22.88, 23.37, 24.61 and 26.51 ppm [40,42] and also long chain branches which observed at about 22.92, 27.89, 29.59, 30.44, 32.23 ppm [41,42]. Additionally, higher pressure significantly increased both the crystallinity and the  $M_n$  values of the resulting polymer (Table 1).

#### 4. Conclusion

The prepared FI-like Ni-based catalysts introducing naphtholato imine group ligands displayed moderate ethylene polymerization activities. There is optimum molar ratios of about [MAO]:[Ni] = 1500:1 for catalyst **2** to reach the highest activity while the activity of catalyst **3** linearly increased by increasing MAO in the range studied. The optimum activity of the catalysts was obtained between 25 and 30 °C. Coexistence of two bulky groups at the *ortho* position to the naphthoxy oxygen and on the nitrogen atom of imine in catalyst **3** led to provide PE with the higher activity as well as higher molecular weight at the expense of lower thermal stability. Higher temperature could profoundly affect the crystallinity of the resulted polymer. A reasonable mechanism for this occurrence is proposed.

#### References

- [1] Sinn H, Kaminsky W, Vollmer HJ, Woldt R. Living polymers on polymerization with extremely productive Ziegler catalysts. *Angew Chem Int Ed* 1980;19:390–2.
- [2] Sinn H, Kaminsky W. Ziegler-Natta catalysis. *Adv Organomet Chem* 1980;18:99–149.
- [3] Hoff R, Mathers RT. Handbook of transition metal polymerization catalyst. Wiley-VCH; 2010.
- [4] Damavandi S, Ahmadjo S, Sandaroos R, Zohuri GH. FI catalyst for polymerization of olefin. In: De Souza Gomes Ailton, editor. *Polymerization*. InTech Publication; 2012. p. 117–44 [Chapter 6].
- [5] Chadwick JC, Duchateau R, Freixa Z, Van Leeuwen PWNM. Homogeneous catalysts. Weinheim, Germany: Wiley-VCH; 2011.
- [6] Smith JA, Brintzinger HH. Ansa-metallocene derivatives. Influence of an interannular ethylene bridge on the reactivity of titanocene derivatives. *J Organomet Chem* 1981;218:159–67.
- [7] Wild FRWP, Zsolnai L, Huttner G, Brintzinger HH. Ansa-metallocene derivatives. Synthesis and molecular structures of chiral ansa-titanocene derivatives with bridge tetrahydroindenyl ligands. *J Organomet Chem* 1982;232:233–47.
- [8] Ewen JA. Mechanisms of stereochemical control in propylene polymerizations with soluble Group 4B metallocene/methylalumoxane catalysts. *J Am Chem Soc* 1984;106:6355–64.
- [9] Ewen JA, Jones RL, Razavi A, Ferrara JD. Syndiospecific propylene polymerizations with Group 4 metallocenes. *J Am Chem Soc* 1988;110:6255–6.
- [10] Canich JAM. (Exxon Chemical Patents, Inc.) Process for producing crystalline polyalpha-olefins with a monocyclopentadienyl transition metal catalyst system; 1991, US Patent 5026798.
- [11] Canich JAM, Licciardi GF. (Exxon Chemical Patents, Inc.) Mono-Cp heteroatom containing group IVB transition metal complexes with MAO: supported catalyst for olefin polymerization; 1991, US Patent 5057475.
- [12] Canich JAM. (Exxon Chemical Patents, Inc.) Olefin polymerization catalysts; 1991, Eur. Patent 0420436.
- [13] Johnson LK, Killian CM, Brookhart M. New Pd(II)- and Ni(II)-based catalysts for polymerization of ethylene and  $\alpha$ -olefins. *J Am Chem Soc* 1995;117:6414–5.
- [14] Small BL, Brookhart M, Bennett AMA. Highly active iron and cobalt catalysts for the polymerization of ethylene. *J Am Chem Soc* 1998;120:4049–50.
- [15] Small BL, Brookhart M. Iron-based catalysts with exceptionally high activities and selectivities for oligomerization of ethylene to linear  $\alpha$ -olefins. *J Am Chem Soc* 1998;120:7143–4.
- [16] Britovsek GJP, Gibson VC, Kimberley BS, Maddox PJ, McTavish SJ, Solan GA, et al. Novel olefin polymerization catalysts based on iron and cobalt. *Chem Commun* 1998:849–50.
- [17] Damavandi S, Ahmadjo S, Sandaroos R, Zohuri GH. FI catalyst for polymerization of olefins. In: De Souza Gomes Ailton, editor. *Polymerization*. InTech Publication; 2012 [Chapter 6].
- [18] Wang C, Friedrich S, Younkin TR, Li RT, Grubbs RH, Bansleben DA, et al. Neutral nickel(II)-based catalysts for ethylene polymerization. *Organometallics* 1998;17:3149–51.
- [19] Olefin upgrading catalysis by nitrogen-based metal complexes. In: Giambastiani G, C ampora J, editors. *Catalysis by metal complexes V* 36. Springer; 2011.
- [20] Zohuri GH, Damavandi S, Sandaroos R, Ahmadjo S. Ethylene polymerization using fluorinated FI Zr-based catalyst. *Polym Bull* 2011;66:1051–62.
- [21] Khaubunsongserm S, Jongsomjit B, Praserttham P. Bis [N-(3-tert-butylsilyl)ethylene] cyclooctylamine] titanium dichloride activated with MAO for ethylene polymerization. *Eur Polym J* 2013;49:1753–9.
- [22] Makio H, Terao H, Iwashita A, Fujita T. FI Catalysts for olefin polymerization—a comprehensive treatment, 2011; 111:2363–2449.
- [23] Matoishi K, Nakai K, Nagai N, Terao H, Fujita T. Value-added olefin based materials originating from FI catalysis: production of vinylidene Al-terminated PEs, end-functionalized PEs, and PE/polyethylene glycol hybrid materials. *Catal Today* 2011;164:2–8.
- [24] Mitani M, Furuyama R, Mohri J, Saito J, Ishii S, Terao H, et al. Syndiospecific living propylene polymerization catalyzed by titanium complexes having fluorine-containing phenoxy-imine chelate ligands. *J Am Chem Soc* 2003;125:4293–305.
- [25] Makio H, Fujita T. Propylene polymerization with bis(phenoxy-imine) group 4 transition metal complexes. *Bull Chem Soc Jpn* 2005;78:52–66.
- [26] Makio H, Fujita T. Development and application of FI catalysts for olefin polymerization: unique catalysis and distinctive polymer formation. *Acc Chem Res* 2009;42:1532–44.
- [27] Wang Hai-Yu, Zhang Jun, Meng Xia, Jin Guo-Xin. Nickel (II) complexes with  $\beta$ -enaminonetonato chelate ligands: Synthesis, solid-structure characterization and reactivity toward the addition polymerization of norbornene. *J Organomet Chem* 2006;691:1275–81.
- [28] Zhang D, Guo S J, Sun W H, Li T, Yang X. Influence of electronic effect on catalytic activity of salicylaldehyde nickel(II) complexes. *J Polym Sci Part A Polym Chem* 2004;42:4765–74.
- [29] Haiyang G, Zuofeng K, Lixia P, Keming S, Qing W. Drastic ligand electronic effect on anilidoimino nickel catalysts toward ethylene polymerization. *Polymer* 2007;48:7249–54.
- [30] Zohuri GH, Damavandi S, Sandaroos R, Ahmadjo S. Highly active FI catalyst of bis[N-(3,5-dicumylsilyl)ethylene]cyclohexylamino]-zirconium(IV) dichloride for polymerization of ethylene. *Iran Polym J* 2012;19:679–87.
- [31] Damavandi S, Zohuri GH, Sandaroos R, Ahmadjo S. Novel functionalized bis(imino)pyridine cobalt(II) catalysts for ethylene polymerization. *J Polym Res* 2012;19:9796–800.
- [32] Ahmadjo S, Zohuri GH, Damavandi S, Sandaroos R. Comparative ethylene polymerization using FI-like zirconium based catalysts. *React Kinet Mech Catal* 2010;101:429–42.
- [33] Damavandi S, Galland GB, Zohuri GH, Sandaroos R. FI Zr-type catalysts for ethylene polymerization. *J Polym Res* 2011;18:1059–65.
- [34] Justino J, Dias AR, Ascenso J, Marcues MM, Tait PJT. Polymerization of ethylene using metallocene and aluminoxane systems. *Polym Int* 1997;44:407–12.
- [35] Brandrup J, Immergut EH. *Polymer handbook*, 3rd ed., vol. VII, New York: Wiley; 1989. p. 1–7.
- [36] Blatt AH. *Org Syn* 1942;22:63 [Wiley, New York].
- [37] Arnold PL, Natrajan LS, Hall JJ, Bird SJ, Wilson C. Symmetric and asymmetric samarium alkoxide derivatives of bridging sulfur biphenolate and binaphtholate ligands; synthetic, structural, and catalytic studies. *J Organomet Chem* 2002;647:205–15.
- [38] Gates DP, Svejda SA, Onate E, Killian CM, Johnson LK, White PS, et al. Synthesis of branched polyethylene using ( $\alpha$ -diimine)nickel(II) catalysts: influence of temperature, ethylene pressure, and ligand structure on polymer properties. *Macromol* 2000;33:2320–34.
- [39] Popeney C, Guan Z. Ligand electronic effects on late transition metal polymerization catalysts. *Organometallics* 2005;24:1145–55.
- [40] Galland GB, Quijada R, Rojas R, Bazan G, Komon ZJA. NMR study of branched polyethylenes obtained with combined Fe and Zr catalysts. *Macromolecules* 2002;35:339–45.
- [41] Linderman L, Adams NO. Carbon-13 nuclear magnetic resonance spectrometry. Chemical shifts for the paraffins through C9. *Anal Chem* 1971;43:1245–52.
- [42] Galland GB, DeSouza RF, Mauler RS, Nunes FF.  $^{13}\text{C}$  NMR determination of the composition of linear low-density polyethylene obtained with [3-Methylallyl-nickel-diimine]PF6 complex. *Macromolecules* 1999;32:1620–5.